ANNUAL REPORT 2007

Meeting date: June 12, 2007

Multi-phase asymmetric fluid flow and inclusion entrapment in the slab mold

Go-Gi Lee
(Visiting Scholar from POSTECH, South Korea)
Brian G. Thomas
(Wilkins Professor of Mechanical Engineering)

Department of Mechanical Science & Engineering
University of Illinois at Urbana-Champaign

Acknowledgements

- Prof. Seon-Hyo Kim
- POSCO -
  especially Drs Joo Choi, Ho-Jung Shin
- Continuous Casting Consortium at UIUC
- Dr Joydeep Sengupta
- Former Graduate Students –
  Quan Yuan, Sana Mahmood

Outline

- Background: origin of defects
- Water model expeiments:
  - Measure argon bubble size entering nozzle
  - Model bubble size distribution in mold
- Computational model
  - Nozzle and Mold
  - Effect of gas flow rate and asymmetric flow
- Plant measurements
  - Nail board
  - Internal inclusions capture locations

Background

Mechanism of defect formation from particle entrapment

1. Gas injection and bubble formation in nozzle
2. Transport of particles (bubbles & inclusions) by flow
3. Inclusions attached to bubbles during transport
4. Bubbles and inclusions entrapped in strand
   - Near meniscus (by hooks)
   - At solidification front (stagnation)
5. Entrapped bubble elongates during rolling and expands during annealing (re-heat) to create blister
5. Entrapped inclusions stretch during rolling to create slivers

Background

1. Gas injection and bubble formation in nozzle

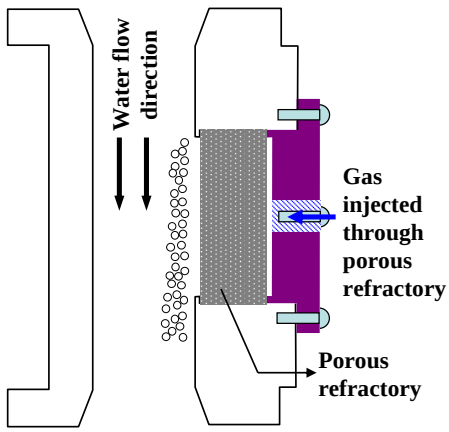

Bubble investigation in water model nozzle

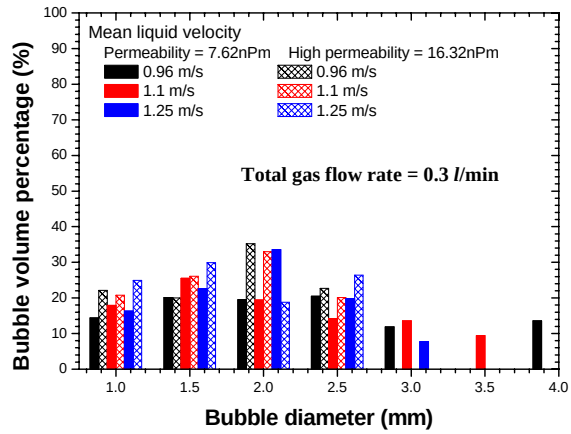

Measured size distribution

Background

2. Particle Transport in Mold by Fluid Flow

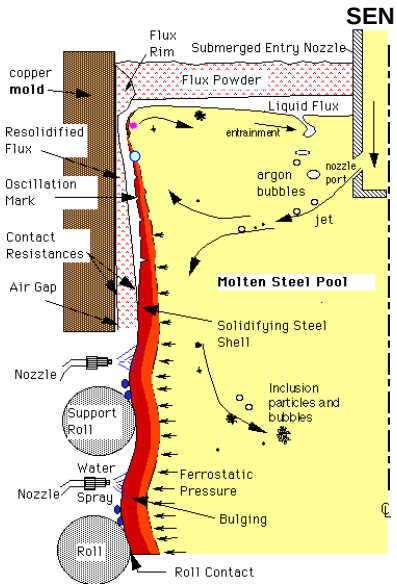

"Continuous Casting Consortium website", ccc.me.uiuc.edu

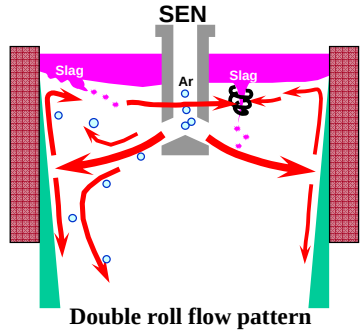

Double roll flow pattern

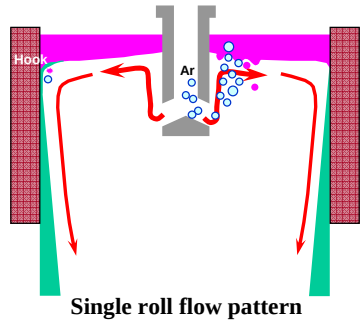

Single roll flow pattern

Entrained Slag Inclusions

Gas Bubbles

Parameters controlling Mold Flow

- Slab depth and width
- Casting speed
- Argon flow rate
- Nozzle shape
  - angle and size of outport
  - nozzle bore diameter
- Submergence depth
- Electromagnetic force

Background

3. Inclusion attached to bubbles during transport

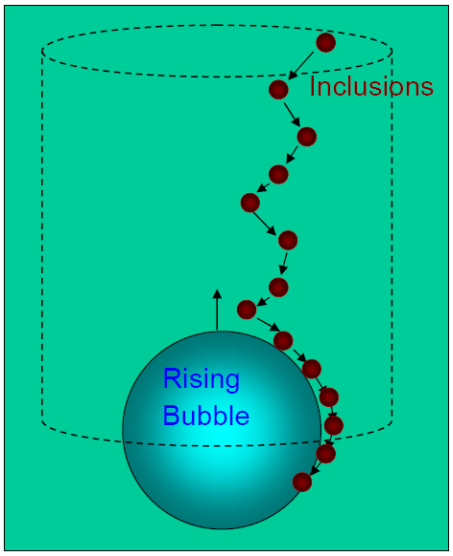

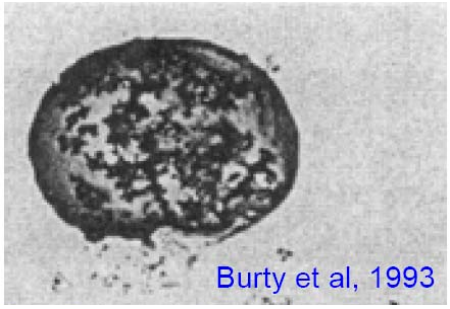

Particle trajectory through molten steel

1. Collision / oscillation
2. Sliding (time for film drainage)
3. Stable attachment

Attachment probability, Pc

$$Pc = \frac{\#\ particles\ attached}{\#\ particles\ in\ column}$$

Background (4 videos)

4. Bubbles and inclusions entrapped in strand

Pitting after 2mm scarfing

Water experiment conditions
- Water flow rate: 36.8 l/min
- Gas flow rate: 9 l/min

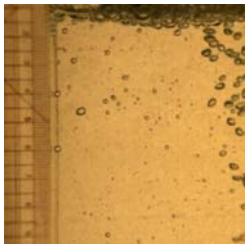

Bubble motion in meniscus region (water model)

OM

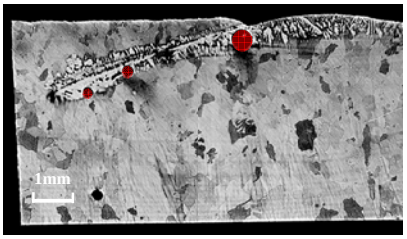

Bubble trapped near meniscus (hook)

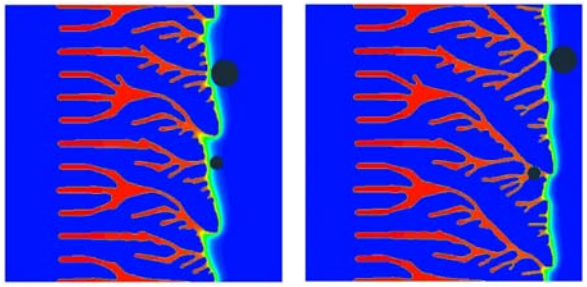

Capture at solidification front

Both captured **(only if stagnant)** Both pushed

A. Chang & J. Dantzig, UIUC, 2006

Background

5. Entrapped bubble elongates during rolling and expands during annealing

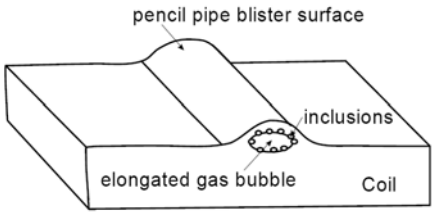

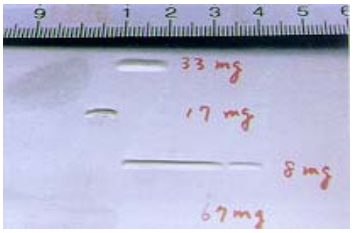

Blister caused by bubble (coil)

5. Entrapped inclusions stretch into slivers

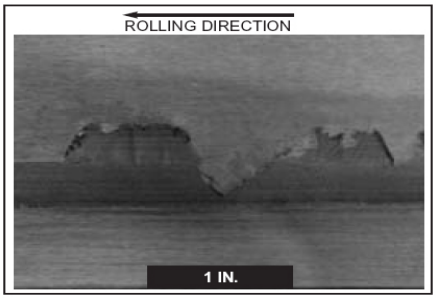

Sliver caused by non-metallic inclusion (coil)

Origin of Different-Shaped void defects in Product

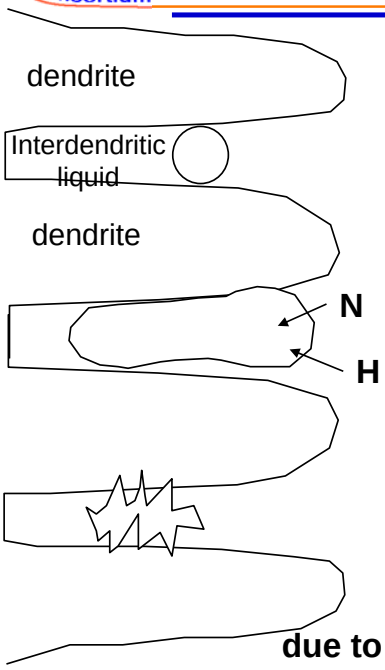

Spherical void

Due to entapped gas bubble eg. argon

Elongated void

Due to Bubble growth during solidification due to preciptation of supersaturated dissolved gas, Eg. H, N)

Jagged void

Micro-porisity, shrinkage cavity due to lack of liquid feeding into interdendritic space

Water Model Apparatus (1/3 scale)

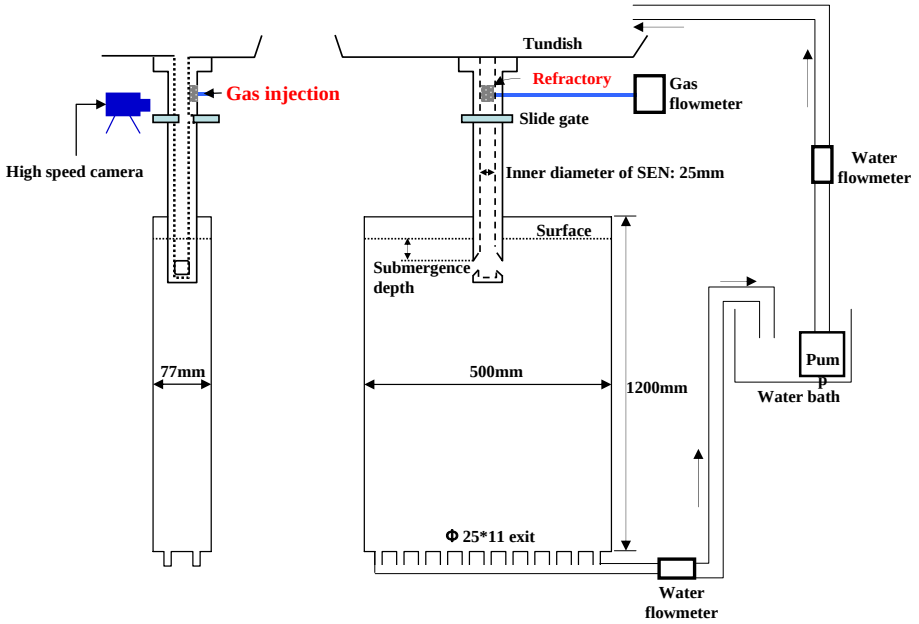

Size of MgO porous refractory brick piece: 14mm(W)*44mm(L)*17mm(D)

Water model experiments to measure bubble size entering upper tundish nozzle

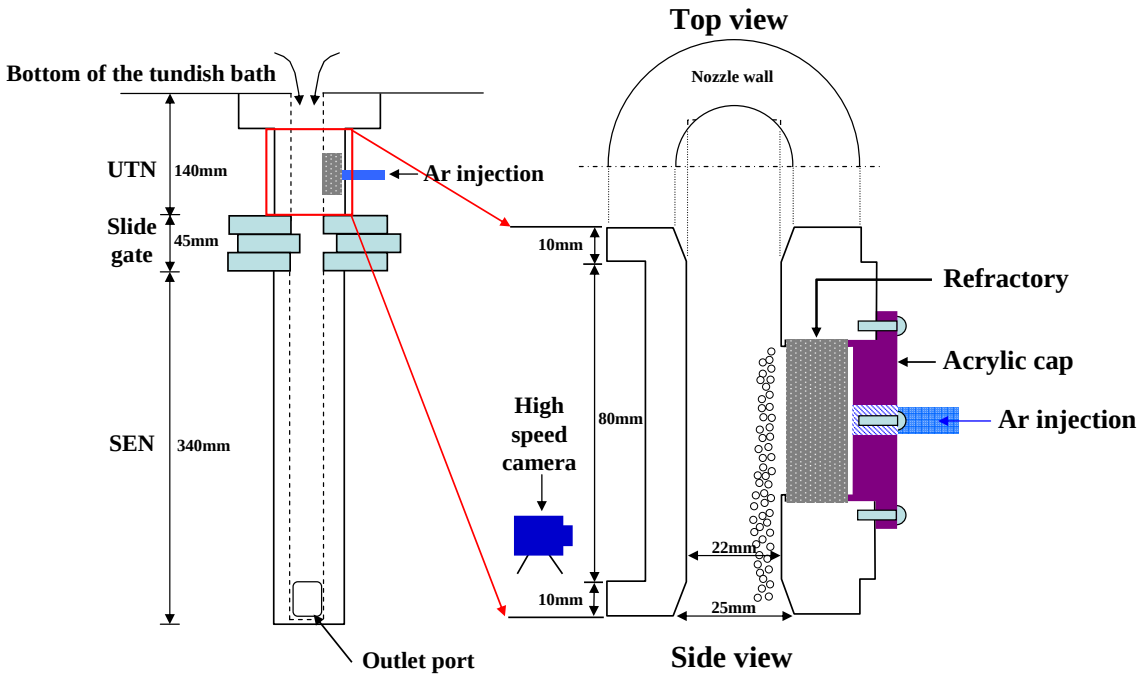

Gas Flow Rate Ratio caused Surface Area of Refractory

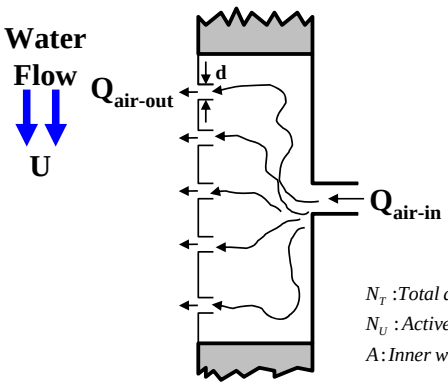

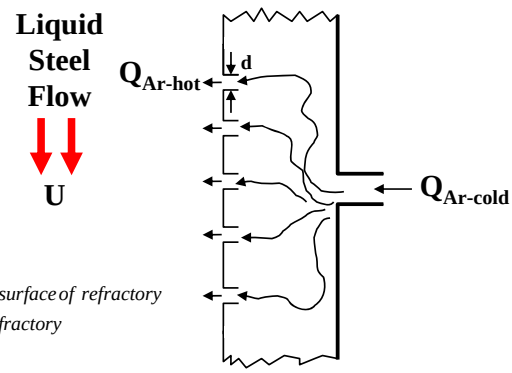

N_T : Total active sites on inner wall surface of refractory
N_U : Active sites per unit area of refractory
A : Inner wall area of refractory

$$Q_{air-out} = \frac{Q_{air-in}}{N_{T,W}} = \frac{Q_{air-in}}{N_{U,W} \cdot A_W}$$

< Schematic of water model experiment >

$$Q_{Ar-hot} = \frac{\beta \cdot Q_{Ar-cold}}{N_{T,S}} = \frac{\beta \cdot Q_{Ar-cold}}{N_{U,S} \cdot A_S}$$

< Schematic of steel caster >

$$\frac{Q_{Ar-hot}}{Q_{air-out}} = \beta \frac{A_W}{A_S} \frac{Q_{Ar-cold}}{Q_{air-in}}$$

β : Ar gas expansin coefficient
A_W / A_S : Surface area ratio of two refractory *
*) see the appendix 1

Comparison of Mean Active Sites between Flowing and Stagnant Flow

Test conditions
- **Low permeability (7.52nPm)**
- **Mean liquid velocity: 1.25 m/s**
- **Total gas flow rate = 0.1 *l*/min**
- **Camera speed: 4000 frames/s**

t=0 **t=0.25ms** **t=0.5ms**

< Example of experiment photograph series >

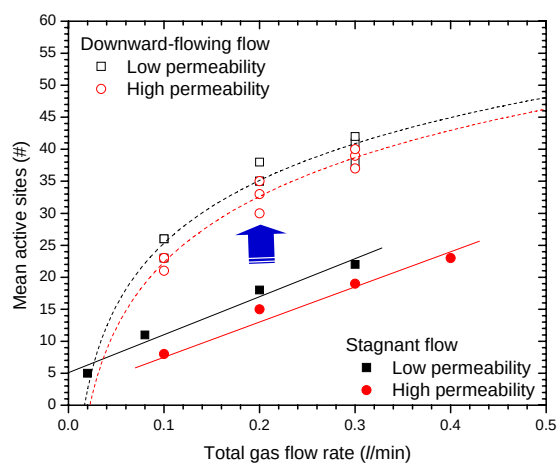

- **Active sites in downward flow are about 2 times those in stagnant flow**
- **Gas flow rate per site of high permeability is slightly higher than that of low permeability in downward-flowing flow at the same total gas flow rate**

Calculation of Total Active Sites in the Steel Caster Nozzle Wall

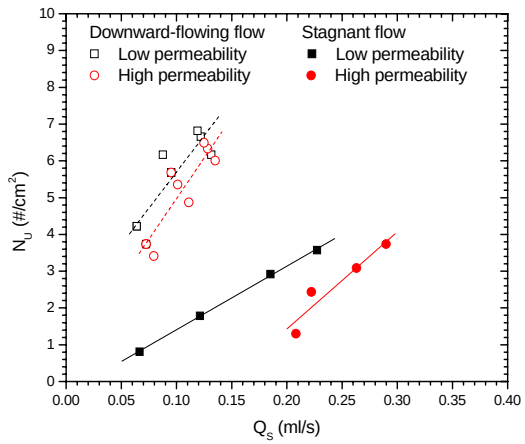

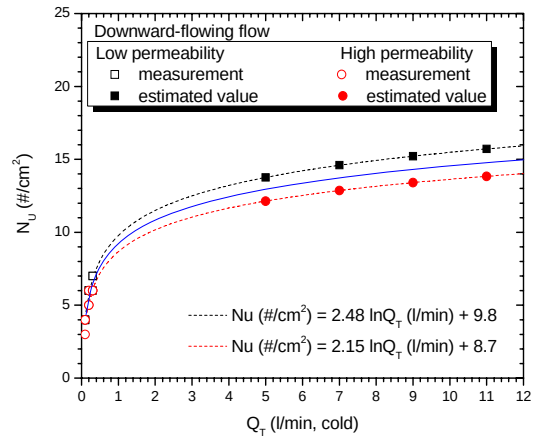

$$Q_S\left(Mean\ gas\ flow\ rate\ per\ site\right)=\frac{Q_T\left(Total\ gas\ flow\ rate\right)}{N_T\left(Total\ active\ sites\right)}$$

	Water Model	Steel Caster
Q_T (Total gas flow rate-cold, l/min)	0.2	7
N_U (Mean active sites per unit area, #/cm^2)	**5.5**	**13.732**
A (Inner wall area of refractory*, cm^2)	6.2	353.4
N_T (Total active sites, #)	**34**	**4853**

***) see appendix 1**

- **Low permeability is much more active sites**

Active sites on porous refractory wall

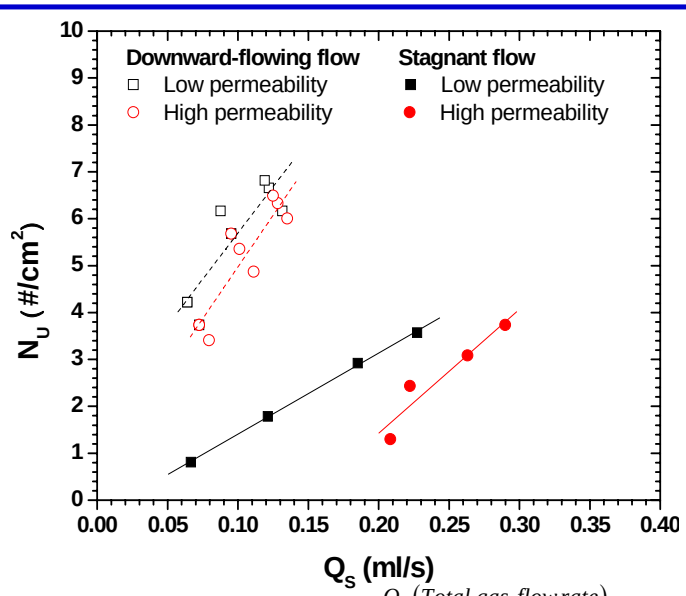

$$Q_S\left(Mean\ gas\ flow\ rate\ per\ site\right)=\frac{Q_T\left(Total\ gas\ flow\ rate\right)}{N_T\left(Total\ active\ sites\right)}$$

- **Lower permeability has higher active sites**

Calculation of total active sites in the steel caster nozzle wall

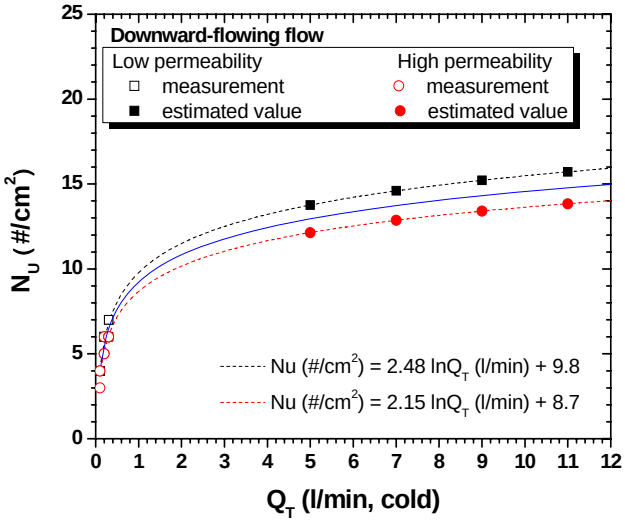

	Water Model	Steel Caster
Q_T (Total gas flow rate-cold, l/min)	0.2	7
N_U (Mean active sites per unit area, #/cm^2)	**5.5**	**13.732**
A (Inner wall area of refractory*, cm^2)	6.2	353.4
N_T (Total active sites, #)	**34**	**4853**

***) see appendix 1**

Comparison of Estimated Mean Gas Flow Rate per Site between Two Systems

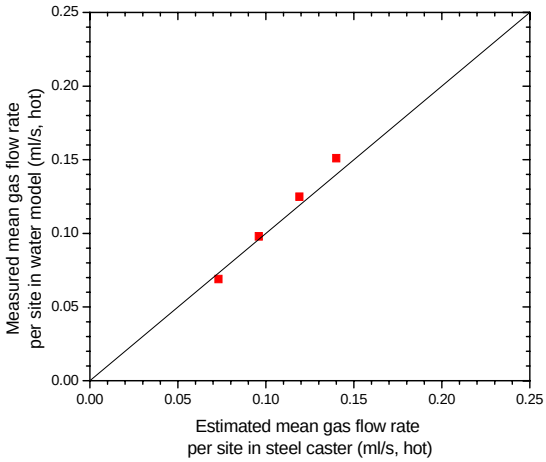

N_U (Mean active sites per unit area on inner wall of refractory) = 2.3154 lnQ_T(SLPM) + 9.2263

Estimated mean gas flow rate per site in steel caster (ml/s, hot)

$$= \frac{\beta \times Q_T\,(cold, l/min)}{A_S^{\,*}\,(cm^2) \times N_U\,(\#/cm^2)}$$

***) A_S = 353.4cm^2, see appendix 1**

	Water Model				Steel Caster			
Q_T (Total gas flow rate-cold, l/min)	0.1	0.2	0.3	0.4	5	7	9	11
β (Gas volume expansion coefficient**)	1				4			
N_T (Total active sites on inner wall area, #)	24	34	40	44	4578	4853	5058	5223
Estimated mean gas flow rate per site (hot, ml/s)	**0.069**	**0.098**	**0.125**	**0.151**	**0.073**	**0.096**	**0.119**	**0.140**

- **Similarity of mean gas flow rate per site between two systems**
  - **It makes the result of water model is meaningful**

Bubble Size Distributions: measured in water model nozzle

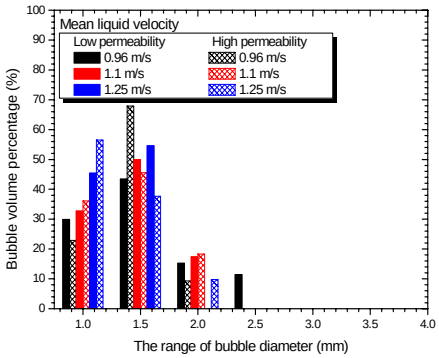

Total gas flow rate = 0.1 *l*/min

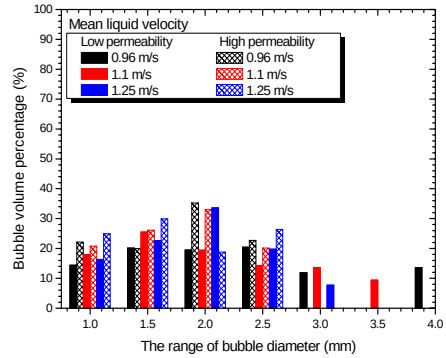

Total gas flow rate = 0.3 *l*/min

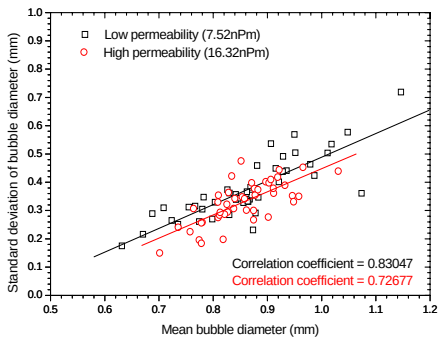

- **Bubble size variations increase with increasing gas flow rate and increasing bubble diameter**

Effect of Liquid Velocity and Gas Flow Rate on Bubble Diameter (water model)

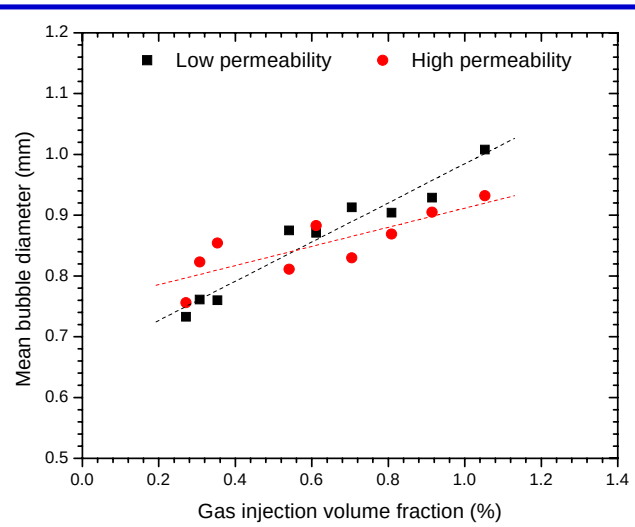

$$Gas\,injection\,volume\,fraction = \frac{Total\ gas\ flow\,rate}{(Total\ gas\ flow\,rate + Liquid\ flow\,rate)} * 100$$

- **The mean bubble size increases with increasing gas flow rate and decreasing liquid velocity**

Comparison of measured and predicted Ar gas bubble size

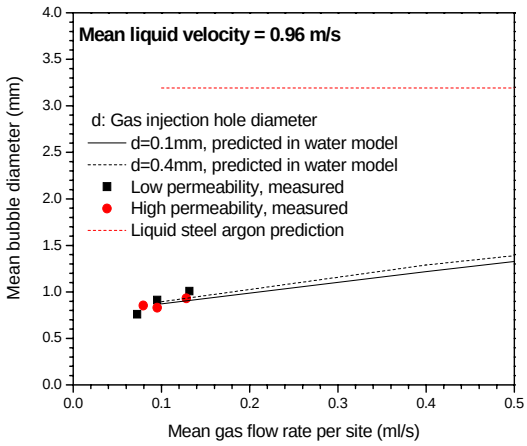

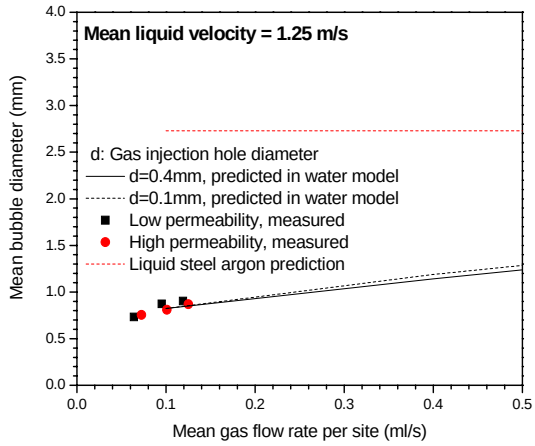

$$Mean\ gas\ flow\ rate\ per\ site = \frac{Total\ gas\ flow\ rate}{Mean\ active\ sites}$$

Bubble size prediction model: $5.2692 \frac{\pi U}{Q_g D_N^{1/7}} \int_{r_e}^{r_d} \left(r^{15/7} (ar + b)^{3/2} + \frac{ar^{22/7}}{2} (ar + b)^{1/2} \right) dr = 2 r_d e_d^{3/2} + \frac{d}{2} - r_e$

Ref.) Bai & Thomas, Met. Trans., 2001

Comparison of estimated Ar bubble size between steel caster and water model using the Bai's prediction

Ref.) Bai & Thomas, Met. Trans., 2001

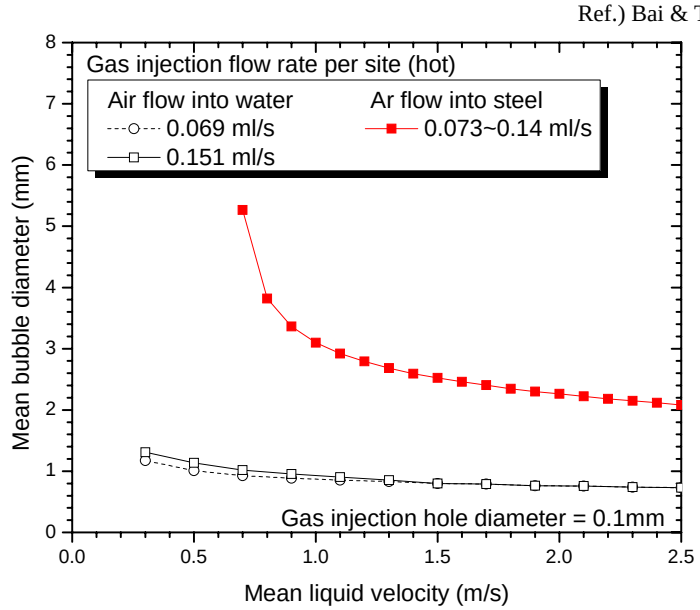

Appendix 1. Surface Area Ratio

Effective length of UTN considered distribution of Ar gas velocity

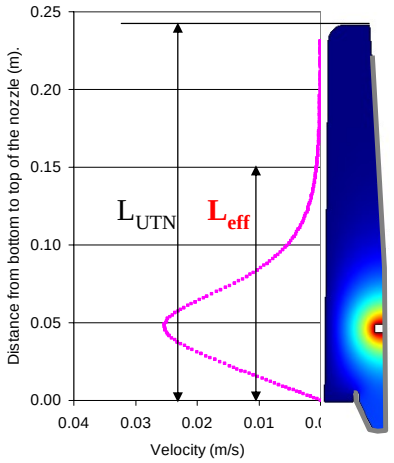

Distribution of Ar gas velocity

B. G. Thomas & Z. Hashisho, CCC Annual Report, 2005

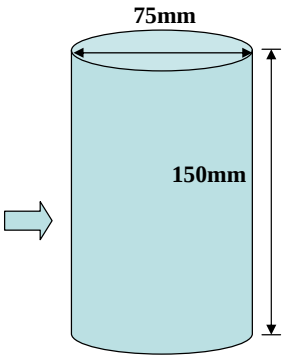

Cylinder-like refractory in actual plant

Surface area (A_S) = 353.4cm^2

VS

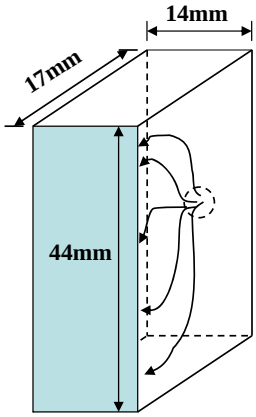

Rectangular refractory fixed in water model

Surface area (A_W) = 6.2cm^2

Rosin-Rammler function for size distribution in FLUENT

$$M_D = \exp\{-(D/\overline{D})^n\}$$

D **: Argon diameter**

M_D **: mass fraction with diameter greater than D**

$\overline{D}$ **: representative bubble diameter when M_D=1/*e***

n : spread parameter

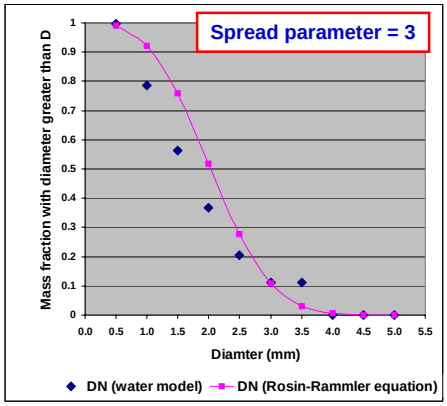

Comparison of DN with water model results and Rosion-Rammler function

→ Well match at spread parameter=3

- **Minimum bubble diameter : 0.112mm**
- **Maximum bubble diameter : 6.4mm**
- **Mean bubble diameter : 2.3mm**
  (Mean liquid velocity = 2m/s)
- **Spread parameter : 3**

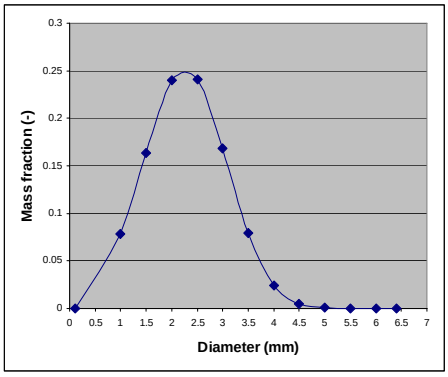

Input data for gas injection in FLUENT (Gas flow rate = 9 SLPM)

- Total gas flow rate (cold) = 9 l/min, (hot) = 36 l/min
- Total gas mass (hot) = 2.68e-07 kg/ms = $36*\rho_g/60*10^{-6}$
- Maximum bubble diameter : 6.4mm
- Mean bubble diameter : 2.3mm
  (Mean liquid velocity = 2m/s)
- Spread parameter : 3

Diameter (mm)	Diameter (m)	M_D	Mass fraction	Mass (kg/ms)	Number of bubbles
0.112	0.00011	1.00E+00	1.15E-04	3.09E-11	94
1	0.001	9.21E-01	7.88E-02	2.11E-08	90
1.5	0.0015	7.58E-01	1.63E-01	4.37E-08	55
2	0.002	5.18E-01	2.40E-01	6.41E-08	34
2.5	0.0025	2.77E-01	2.41E-01	6.46E-08	18
3	0.003	1.09E-01	1.68E-01	4.50E-08	7
3.5	0.0035	2.95E-02	7.92E-02	2.12E-08	2
4	0.004	5.19E-03	2.43E-02	6.50E-09	0
4.5	0.0045	5.59E-04	4.64E-03	1.24E-09	0
5	0.005	3.45E-05	5.24E-04	1.40E-10	0
5.5	0.0055	1.15E-06	3.34E-05	8.93E-12	0
6	0.006	1.95E-08	1.13E-06	3.03E-13	0
6.4	0.0064	4.39E-10	1.91E-08	5.10E-15	0

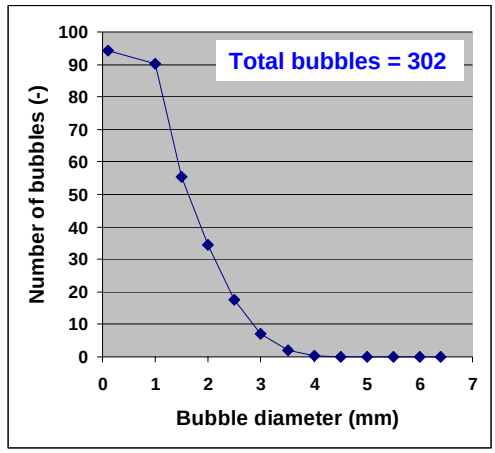

→ The initial positions of bubbles: random position on inner wall upper tundish nozzle
→ Bundle of bubbles (168 bubbles) are continuously injected at every ms
→ Time step is 0.001sec

Nozzle velocity with different gas flow rates

(1sec after injection ~ steady state)

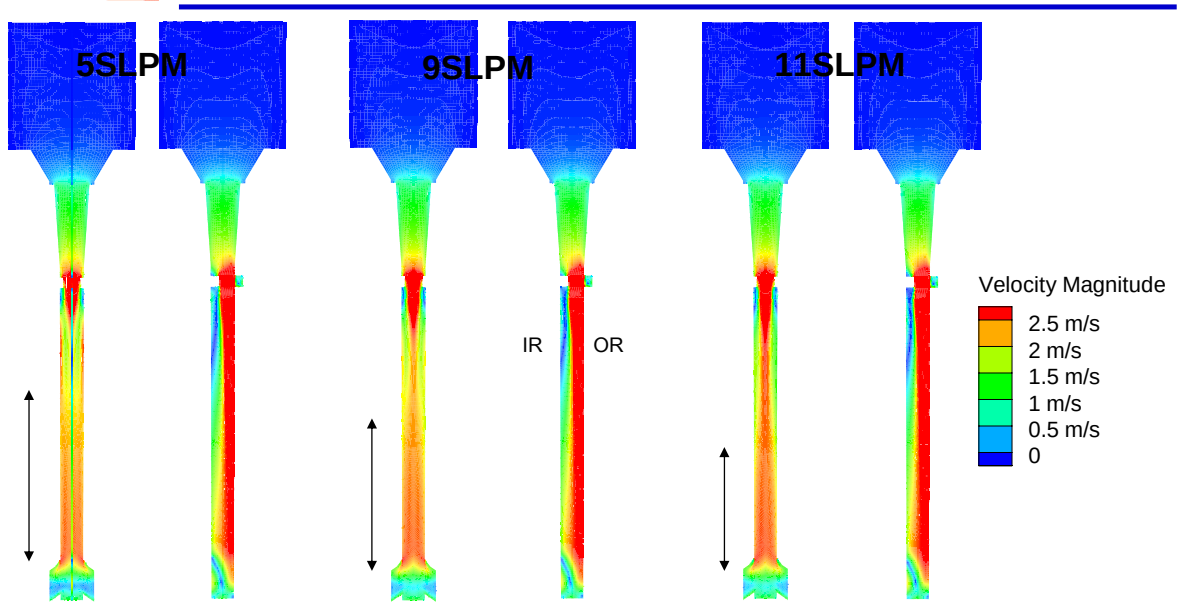

Higher gas flow: higher recirculation zone beneath slide gate
smaller relaxation length of uneven flow due to slide gate

Bubble concentration in nozzle

(1sec after injection ~ steady state)

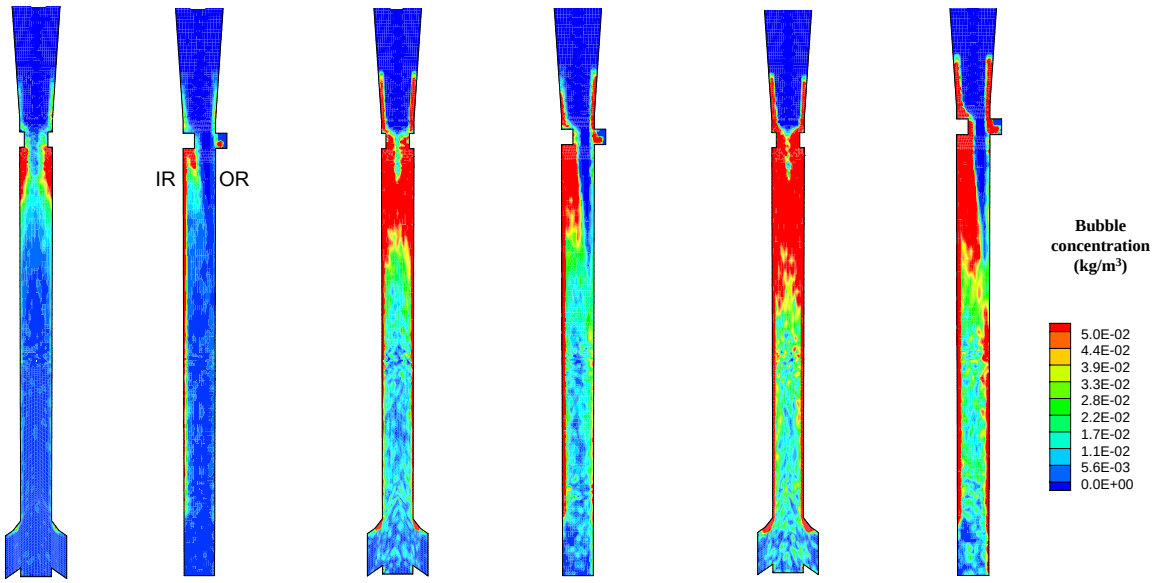

Front view **Side view** **Front view** **Side view** **Front view** **Side view**

Gas flow rate = 5 *l*/min **Gas flow rate = 9 *l*/min** **Gas flow rate = 11 *l*/min**

Two phase fluid flow in nozzle: recirculation regions

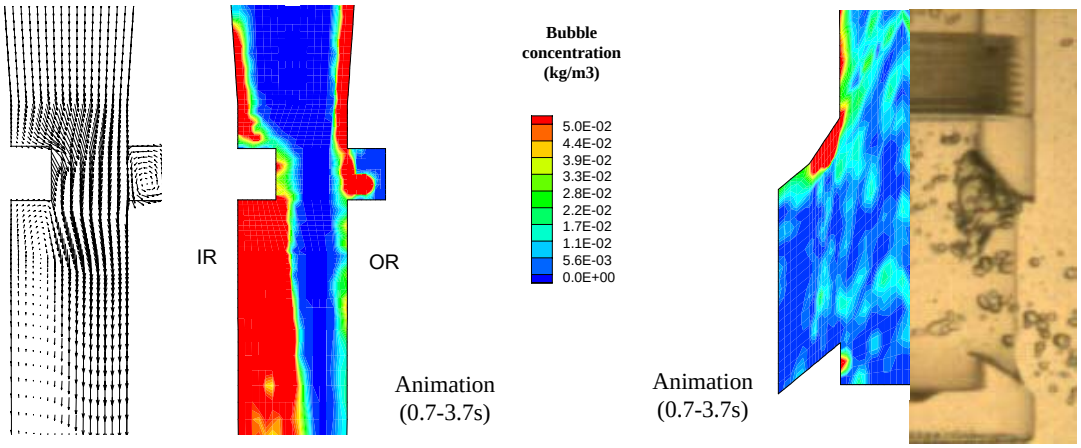

Velocity vector (9 *l*/min) **Bubble concentration (9 *l*/min)** **Computer simulation (9 *l*/min)** **Water modeling**

(1s after injection)

- **Recirculation region**
  → Causes large bubbles

Slide gate region **Outport region**

Velocity distribution at ports

(1sec after injection ~ steady state)

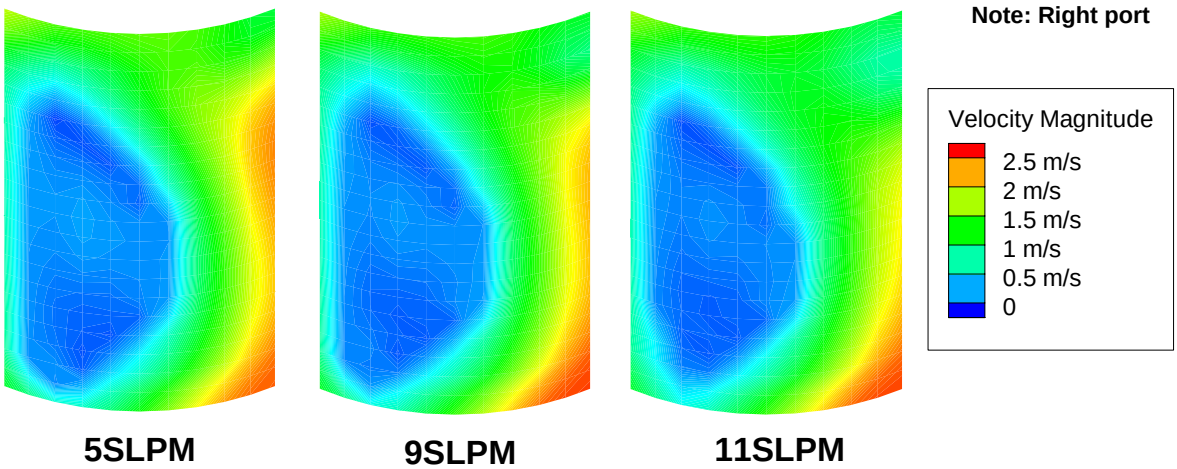

- **Higher gas flow**
  - **increase gas**
  - **decrease the flow velocity at SEN outport**

Bubble concentration at ports

(1sec after injection ~ steady state)

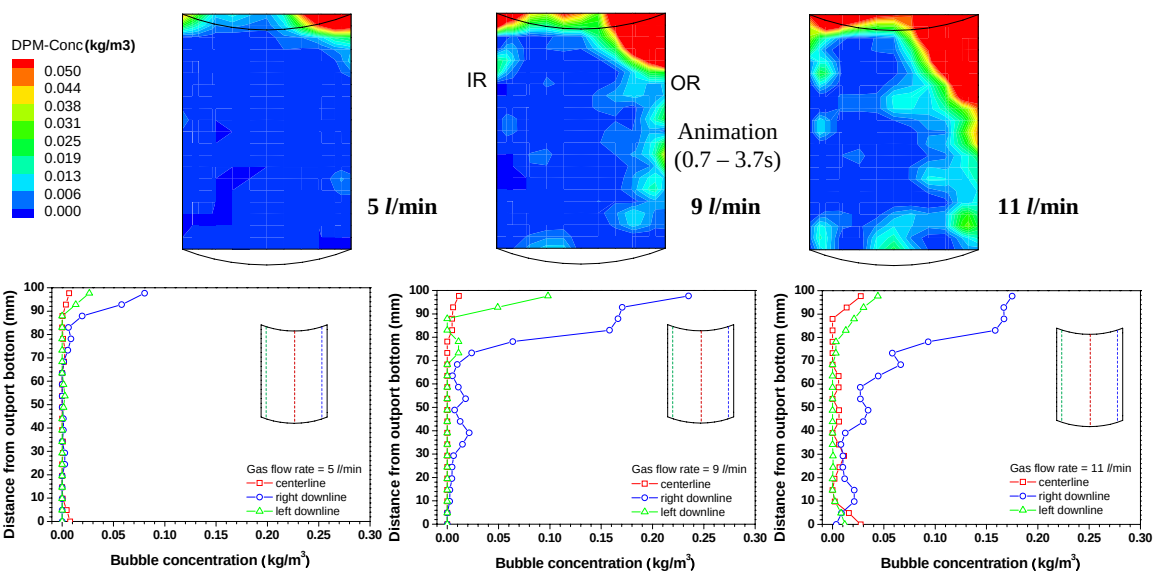

- **Asymmetric flow causes gas flow to exit top corner of nozzle ports**

Comparison of asymmetric flow due to slide gate (single phase simulation)

Steel output = 61.6kg/s

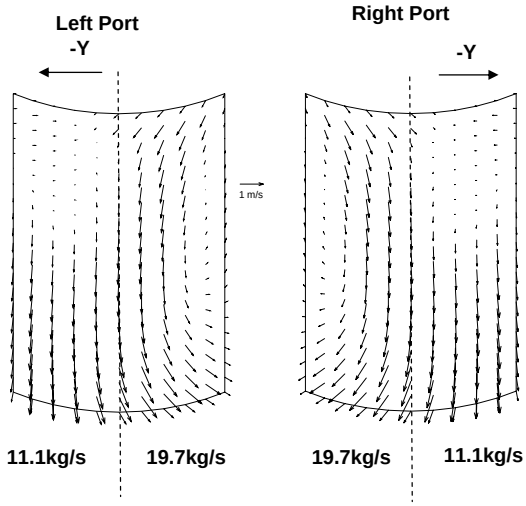

k-ε model simulation
(S. Mahmood, M.S. Thesis, 2006, UIUC)

Steel output = 59.69kg/s

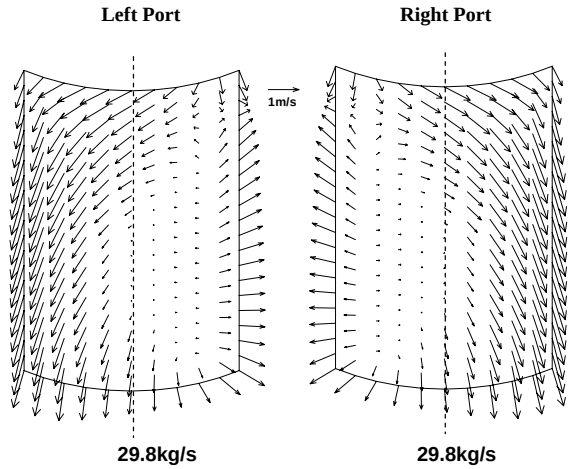

RSM simulation

Cross-sections of mold

- **Simulation conditions**
  - **Slab thickness: 230mm**
  - **Slab width: 1570mm**
  - **Casting speed: 1.46m/min**
  - **Ar gas flow rate: 9*SLPM***
  - **No electromagnetic effect**

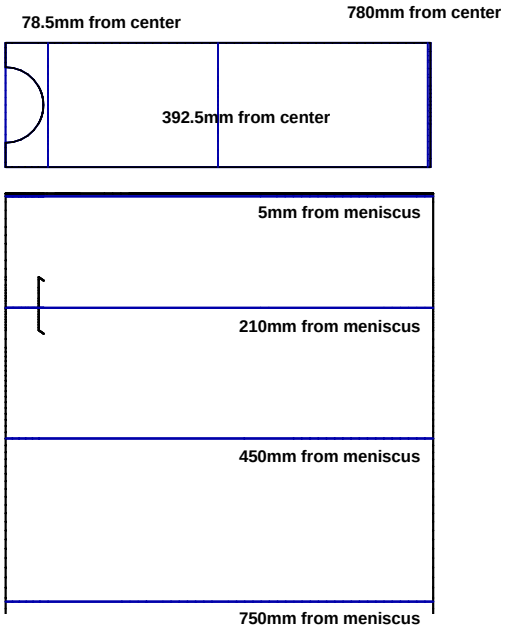

Velocity distribution in mold

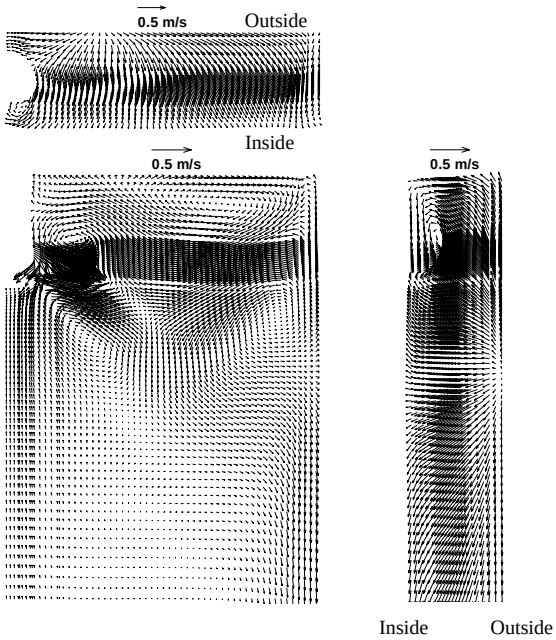

30.4sec

Comparison of velocity magnitude along centerline

Cross-section of 10mm from meniscus

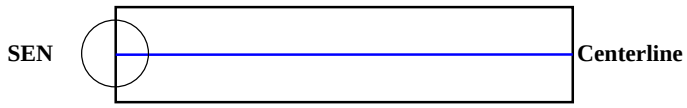

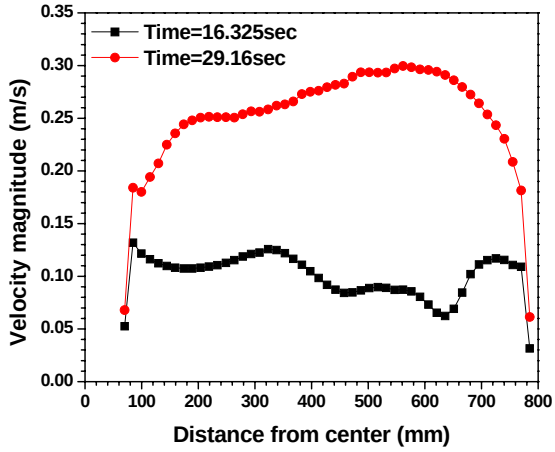

Comparison of velocity magnitude along strand length

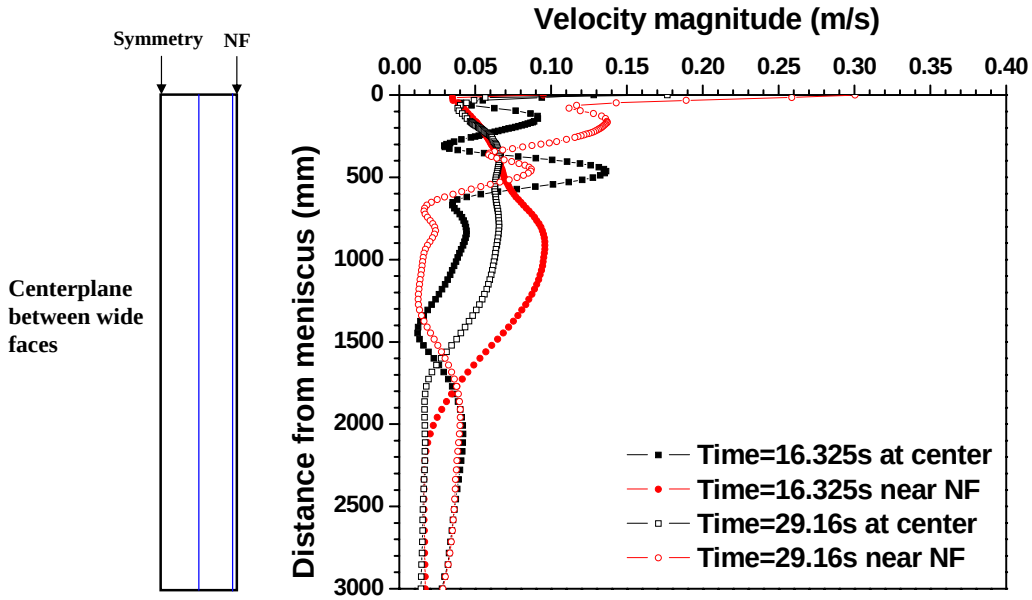

Bubble size distribution in mold

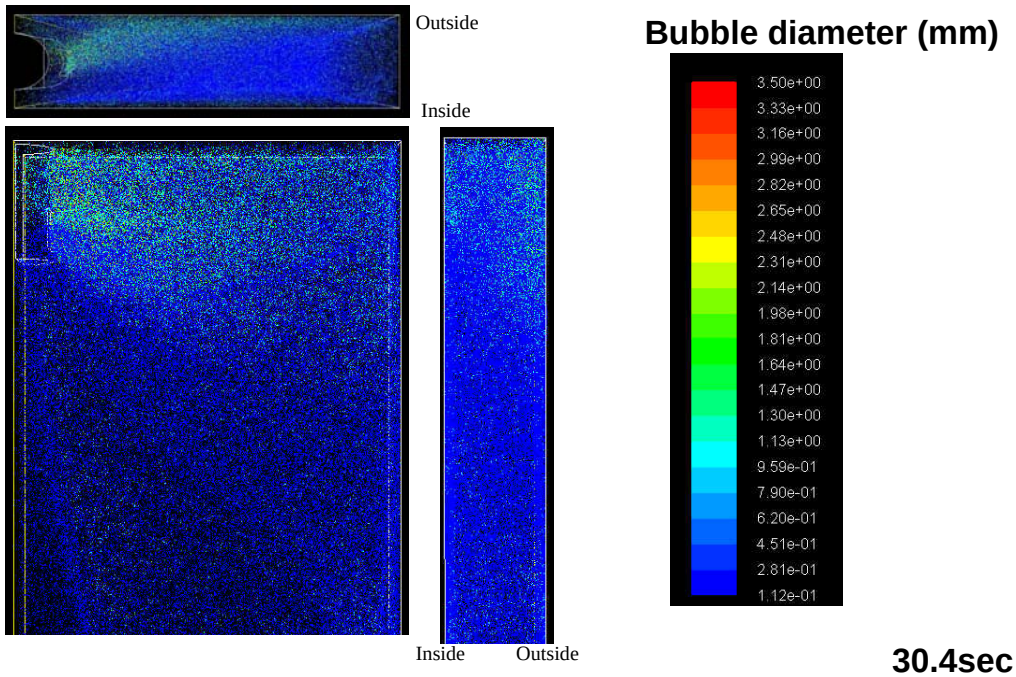

Bubble concentration in mold

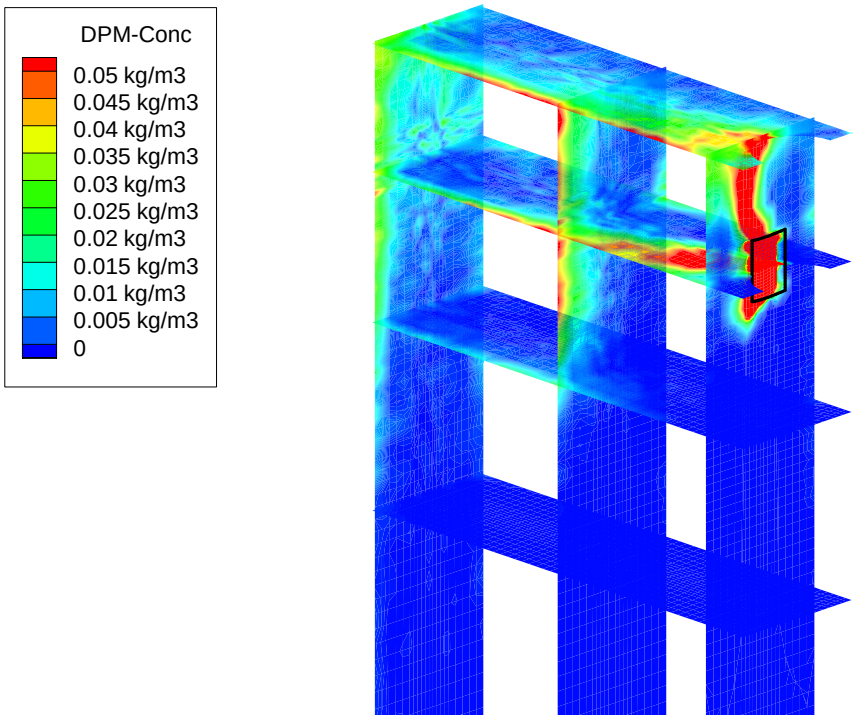

30.4sec

Bubble concentration at different time

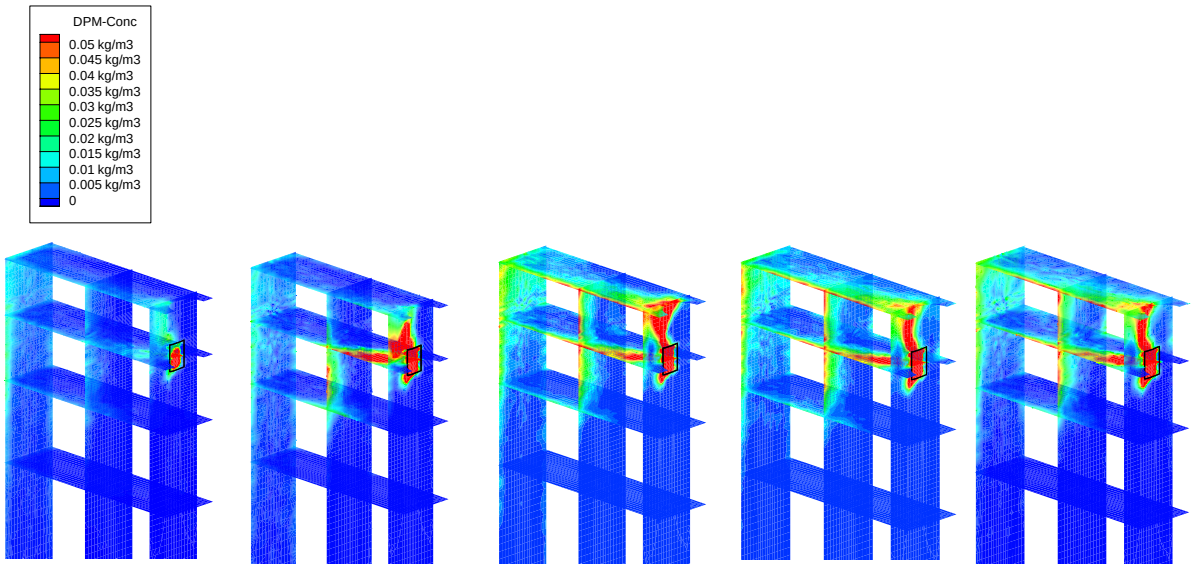

5sec **16.3sec** **20.2sec** **25.2sec** **30.4sec**

Estimated time to reach the steady state

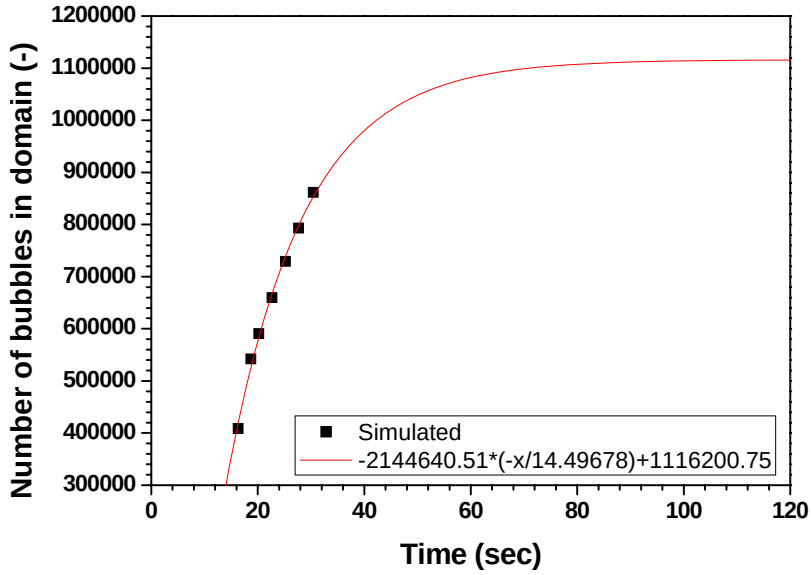

- Simulation will be reached to steady state at 90sec after injection

Bubble concentration in mold for different gas flow rates (2sec after injection)

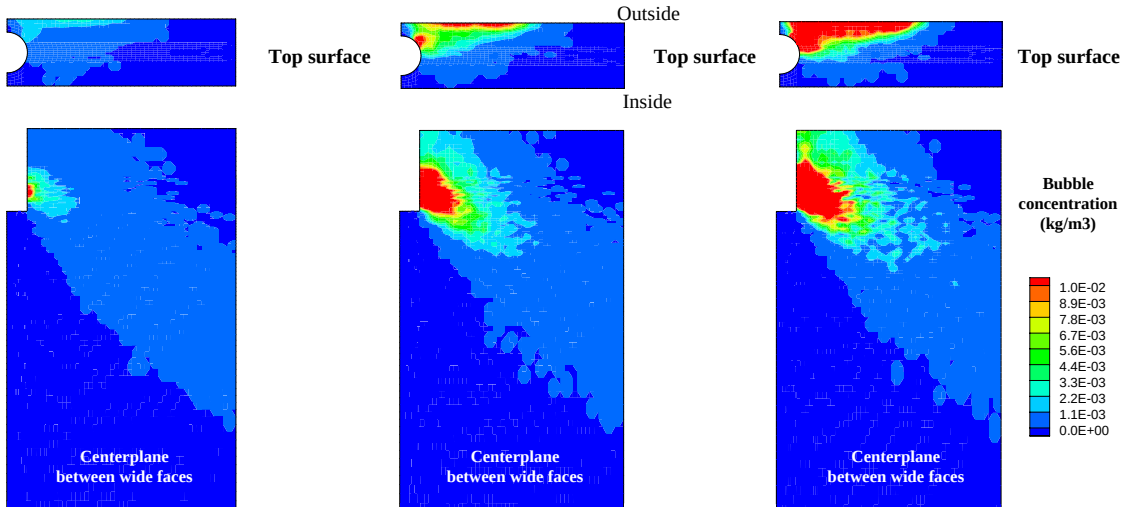

Ar flow rate = 5 *l*/min | Ar flow rate = 9 *l*/min | Ar flow rate = 11 *l*/min

- **Near SEN and top surface has a high bubble concentration**

Plant Experiments (nail-board tests)

2006

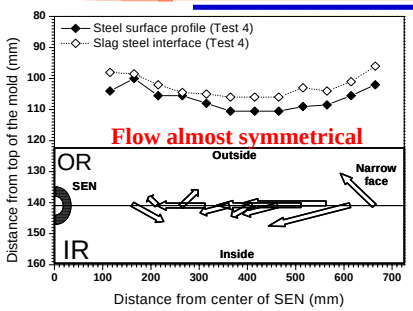

Ar flow rate : 4.58 *l*/min

Ar pressure : 0.74 bar

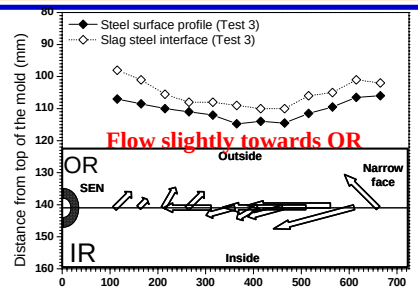

Ar flow rate : 6.18 *l*/min

Ar pressure : 0.80 bar

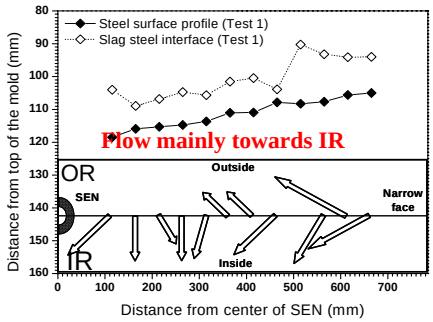

Ar flow rate : 9.60 *l*/min

Ar pressure : 0.97 bar

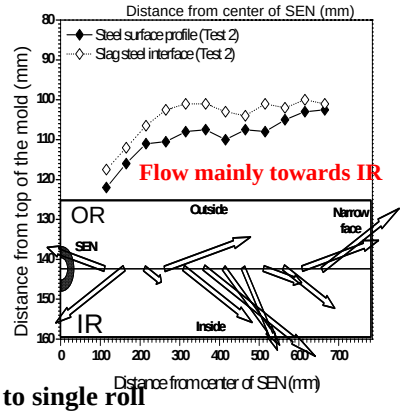

Ar flow rate : 12.20 *l*/min

Ar pressure : 1.03 bar

- **Increasing Ar gas flow causes:**
  1) **flow pattern change from double roll to single roll**
  2) **asymmetric flow (mainly towards inside radius for high Ar flow)**

Particle distribution with depth from slab surface using ultra-sonic analysis

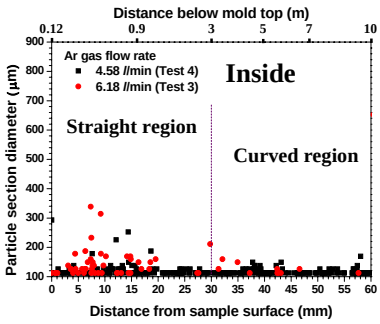

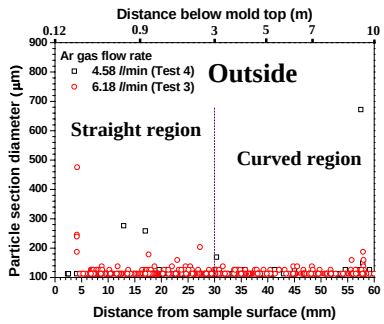

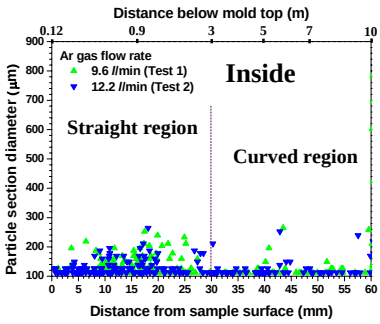

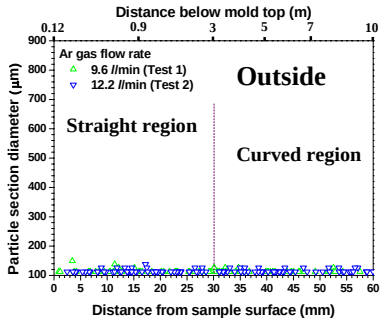

1. **<u>Distance down caster</u>**
   - defects in both straight and curved regions
   → not controlled by surface hooks or by flotation effects
2. **<u>Higher Ar gas flow rate</u>**
   - More defects on IR
   → caused by asymmetric flow between wide faces

Conclusions (modeling results)

- Gas exits upper outside-radius corner of nozzle port (owing to asymmetric flow inside nozzle
- Gas rises up outside radius of mold, causing high gas concentration on top surface (OR)
- Gas rising causes rising flow, which washes particles away from OR (particle entrapment not possible with upward flow, because gas buoyancy assists cross velocity)
- Gas flow across thickness of mold surface carries flow down inside radius (if gas flow rate is high enough)
- Downward flow makes inclusion / bubble entrapment possible (if downward flow velocity matches particle buoyancy)
- Result: increased entrapment on inside radius of wide face at higher gas flow rates, and different bubble size distributions in different locations (according to downward velocity)

Conclusions

- Gas exits upper outside-radius corner of nozzle port (owing to asymmetric flow inside nozzle)
- Gas rises up outside radius of mold, causing top surface to have: high gas concentration at OR and flow towards IR
- Increasing gas flow rate (>9 l/min)
  - Flow towards inside radius, confirmed by nail-board measurements
  - Causes more particles entrapped, especially on inside radius, corresponding to asymmetric flow
  - Straight wall until shell is 30mm thick indicates that most defects are not due to machine curvature, but due to asymmetric flow
- Asymmetric flow towards one face increases entrapment (both frequency and particle size) on that face and decreases entrapment on the opposite face
- Particle entrapment seems mainly due to poor / asymmetric fluid flow conditions